

Water Resources Research



RESEARCH ARTICLE

10.1029/2020WR028706

Key Points:

- Position of reaction fronts for nitrate and acidification in aquifers checked after 20+ years
- Acidification of soil and groundwater still strong, despite reductions of atmospheric input
- Nitrate front has moved very slowly over last 20 years but denitrification products have migrated into lower aquifer

Supporting Information:

Supporting Information may be found in the online version of this article.

Correspondence to:



G. J. Houben,
georg.houben@bgr.de

Citation:

Houben, G. J., Post, V. E. A., Gröger-Trampe, J., Pesci, M. H., & Sültenfuß, J. (2021). On the propagation of reaction fronts in a sandy aquifer over 20+ years: Lessons from a test site in northwestern Germany. *Water Resources Research*, 57, e2020WR028706. <https://doi.org/10.1029/2020WR028706>

Received 1 SEP 2020
 Accepted 23 JUL 2021

On the Propagation of Reaction Fronts in a Sandy Aquifer Over 20+ Years: Lessons From a Test Site in Northwestern Germany

Georg J. Houben¹ , Vincent E. A. Post¹, Jens Gröger-Trampe², María H. Pesci³ , and Jürgen Sültenfuß⁴

¹Federal Institute for Geosciences and Natural Resources (BGR), Hannover, Germany, ²State Authority for Mining, Energy and Geology (LBEG), Hannover, Germany, ³Institute of Hydrology and Water Resources Management, Leibniz University, Hannover, Germany, ⁴Institute for Environmental Physics, University of Bremen, Bremen, Germany

Abstract Despite reduction measures, nitrate and aluminum concentrations remain high in aquifers in northwestern Europe. To evaluate the effectiveness of groundwater protection policies, the long-term fate of these contaminants in groundwater needs to be understood. The groundwater catchment of the Haren water works, NW Germany, was characterized hydrogeochemically in the late 1990s, which provides an opportunity to study the solute fronts over a two-decade period and conduct a post-audit of the predicted front movement. Results indicate that, despite a significant reduction of the atmospheric acid loads, the acidification of soil and groundwater at the forest site persists. Removal of sorbed aluminum is required to induce a noticeable improvement, which will take at least several decades. The unexpected appearance of nitrate at the site, caused by a land use change in 1998, highlights the need for long-term monitoring. Core data at the agricultural site show that the denitrification front has moved very little between 1998 and 2017, in accordance with previous forecasts. Denitrification by-products, mainly sulfate and nitrogen, have migrated from the upper into the lower aquifer. A reactive transport model demonstrated how the link between the regional groundwater flow, pyrite oxidation, and the temporal variability of the nitrate concentration in recharge water, as reconstructed from age tracers, result in the observed vertical distribution of sulfate and nitrogen. This study demonstrates how long-term monitoring, aided by model-based data interpretation, can be used to successfully study and predict the fate of contaminants in groundwater.

1. Introduction

The negative effects of diffuse contaminant sources on groundwater quality in northwestern Europe and other parts of the world gained public and scientific attention in the early 1980s. These include the acidification of soil and groundwater from atmospheric inputs (“acid rain”), and the resulting environmental problems due to the mobilization of aluminum (e.g., Bouwman et al., 2002; Galloway et al., 1976; Henriksen & Kirkhusmo, 1982; Hrkal, 2001; Johnson et al., 1981). In Northern Germany, there are several well-documented cases of soil and aquifer acidification (Beyn et al., 2014; Franken et al., 2009; Houben et al., 2001, 2019; Lükewille & van Breemen, 1992; Meesenburg et al., 1995). Another effect is the contamination of groundwater through intensive agriculture, especially by nitrate. Although this problem had already been identified in the 1960s (Keller & Smith, 1967; Singh & Sekhon, 1979), it became much more prominent from the 1980s (e.g., Kölle et al., 1982; Korom, 1992; Lee & Weber, 1982; Luehr & Muschack, 1983; Overrein, 1983; Postma et al., 1991; Smith et al., 1991; Trudell et al., 1986). Some of the earlier studies involved the application of hydrogeochemical reaction models (Appelo, 1985; Frind et al., 1990) that simulated the observed geochemical patterns and predicted the future hydrochemical development. Through these studies, it became clear that the propagation of acidification and nitrate through the subsurface is buffered by reactions with soil and aquifer matrix material (e.g., Rivett et al., 2008).

Nowadays, there is little talk about acid rain in Europe anymore but nitrate contamination of aquifers remains a major issue (Jia et al., 2020; Padilla et al., 2018). There are fears that the denitrification capacity of some aquifers might become exhausted at some point, leading to an uncontrolled breakthrough of nitrate and costly water treatment (Wilde et al., 2017). Locating the denitrification front is thus a key issue. This requires a depth-specific analysis of both groundwater and the reactive inventory of the aquifer matrix.

© 2021. The Authors.

This is an open access article under the terms of the [Creative Commons Attribution-NonCommercial-NoDerivs License](https://creativecommons.org/licenses/by-nc-nd/4.0/), which permits use and distribution in any medium, provided the original work is properly cited, the use is non-commercial and no modifications or adaptations are made.

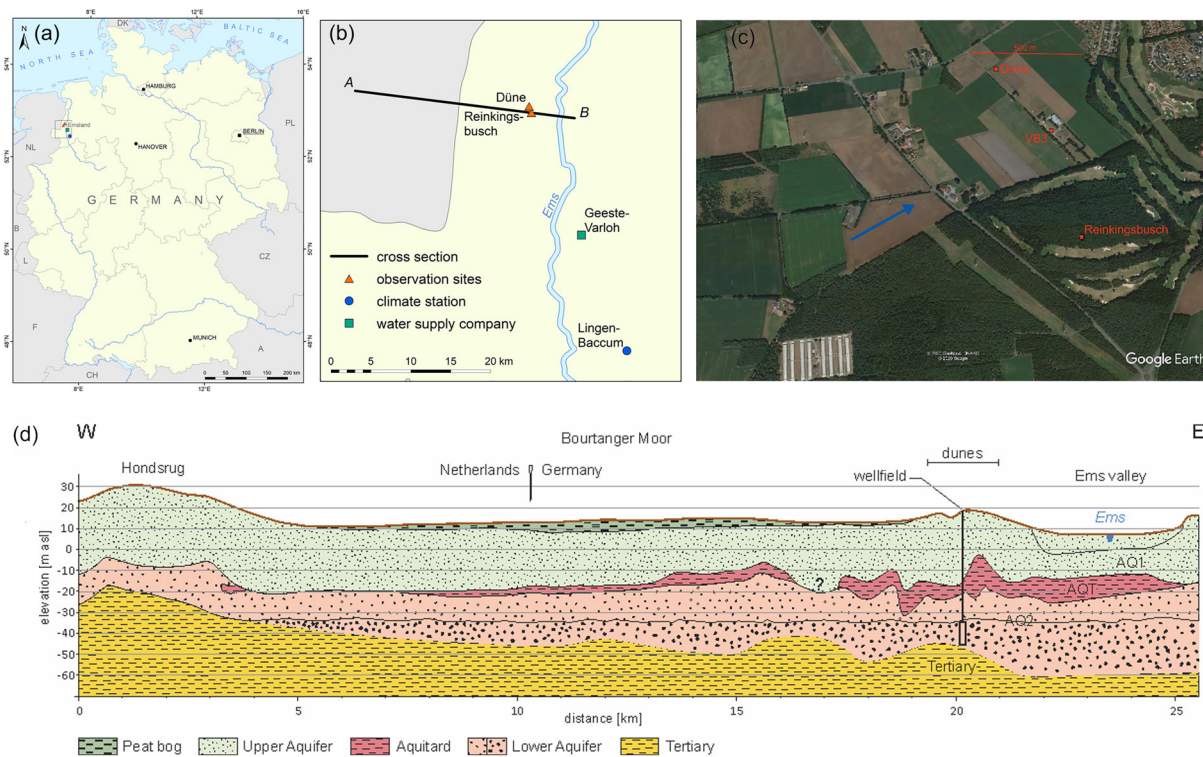


Figure 1. (a) Location map of the Emsland (B = Belgium, NL = Netherlands, PL = Poland, CZ = Czech Republic, A = Austria, DK = Denmark), (b) map showing position of cross section A–B (A = West, B = East), climate station and seat of the water supply company, (c) aerial picture with investigation sites Düne (agriculture), Reinkingsbusch (forest, clearings are the golfing greens) and pumping well VB3, blue arrow = direction of regional groundwater flow (image source Google Earth), (d) schematic geological cross section, based on drilling logs provided by the water supply company, the State Authority for Mining, Energy, and Geology (LBEG) of Lower Saxony and for the Dutch side, taken from the DINOloket repository provided by TNO, Geological Survey of the Netherlands (www.dinoloket.nl).

Because the front moves very slowly, tracking it requires long-term studies, in the order of decades. Studies of this type are therefore rare. Jessen et al. (2017) studied a lithotrophic denitrification front in Denmark for 25 years via repeated depth-specific hydrochemical analysis. They found that nitrate inputs had nearly halved, due to better nutrient management implemented in the late 1980s, but that a plume of the denitrification product sulfate had persisted. The depth to the denitrification front had hardly changed at all. They did not, however, consider drillcore sediment to confirm this. In the absence of repeated core samplings, the accuracy of model predictions on front velocity made in the past remains unchecked.

Both acidification and nitrate pollution were studied in the catchment of the Haren water works in the Emsland region in northwestern Germany (Figure 1) at the end of the 1990s. Groundwater as well as soil and aquifer material were investigated by depth-specific sampling and geochemical analysis (Houben, 2000; Houben et al., 2001). This allowed the delineation of reaction front depths, while reactive transport modeling provided estimates of their propagation velocity. This was done for a pine forest site (Reinkingsbusch), suffering from soil and groundwater acidification and an agricultural site (Düne), suffering from nitrate contamination.

The first objective of this study was to investigate how far the reaction fronts of both aluminum and nitrate have progressed in the Haren sites over the last 22 years. Therefore, both the multilevel observation wells were resampled and new drill cores were collected at both sites. Second, the results provided a chance of assessing the quality of model predictions on front velocities by Houben et al. (2001, 2017), taking into account changes in land use and atmospheric input during the last 22 years.

2. Study Site and Methods

2.1. Study Site

The sites studied here belong to the Emsland region, located at the eastern border of the Bourtanger Moor, where the ombrogenous peat bog gradually transitions to the glaciofluvial deposits of the Ems valley (Figure 1). The boundary between sand and peat is often marked by Holocene dunes. Quaternary glacial and postglacial processes have formed the hydrogeological strata present today (Figure 1). The upper, unconfined aquifer has an average thickness of around 20 m and consists mainly of fine sands, probably deposited during the Drenthe stadium of the Saalian glaciation (0.126–0.30 million years before present [Ma]). The lower, confined aquifer has an average thickness of around 30 m, with an upper sandy part and a lower coarser, gravely part. It was probably deposited during the Elsterian glaciation (0.320–0.400 Ma). A clay-rich aquitard with an average thickness of 5 m separates the aquifers. It formed during the Holstein interglacial (0.325–0.340 Ma). Tertiary clay deposits form the basal aquitard.

The upper aquifer is only used locally by farmers for plot irrigation, which has become more important in the last 5 years due to a series of dry summers. Its hydraulic conductivity ranges around $1\text{--}2 \times 10^{-3}$ m/s, according to pumping tests described in Houben (2000). Groundwater extraction from the lower aquifer for public water supply started in 1961 and became stable at approximately 1.5×10^6 m³/a at around 1985. In the year 2005, the extraction was raised to 2.0×10^6 m³/a. According to pumping tests by Houben (2000), its hydraulic conductivity of $6\text{--}10 \times 10^{-3}$ m/s is significantly higher than the upper aquifer. Close to the pumping wells, current groundwater levels between the aquifers differ by about 2–3 m, with levels in the lower aquifer being lower due to pumping. A detailed description of the region and its geology as well as hydrogeology can be found in Schwan (1987), Houben (2000), and Houben et al. (2001, 2017).

The raised peat bog of the Bourtanger Moor started its growth in the Holocene around 6,500 years ago. Human impact began in the 17th century (Casparie, 1993; Haverkamp, 2011), including drainage, deep plowing and peat mining, and intensified after World War II. The sandy podzolic substrates, east of the peat bog, were in part also drained by deep plowing, intended to break-up the deeper, impermeable bog iron layers. The climate is temperate oceanic with an average rainfall rate of around 800 mm/a and a mean temperature of 8.9°C.

Land use today is dominated by intensive agriculture, especially poultry and pig farming but also maize and potato. Nitrogen loads are very high, ranging between 100 and 120 kg N per hectare of agricultural area, including 20 kg/ha of atmospheric deposition (Haakh, 2017). In combination with the well-drained soils, this has led to widespread nitrate contamination of the shallow aquifers with concentrations of up to 250 mg/l (Houben et al., 2001, 2017). Forestry is mostly restricted to the former dune areas with their podzolic soils, pine being the most common tree type.

The position of the nitrate front in the agricultural site is primarily controlled by the presence of pyrite in the sediment of the upper aquifer (Houben et al., 2001, 2017). The oxidation of pyrite by nitrate (called lithotrophic denitrification) is considered one of the most important controls for nitrate migration in aquifers (Böhlke et al., 2002; Böttcher et al., 1990; Engesgaard & Kipp, 1992; Frind et al., 1990; Houben et al., 2001; Juncher Jorgensen et al., 2009; Kölle et al., 1982; Postma et al., 1991; Vaclavkova et al., 2014; van Beek et al., 1989; Zhang et al., 2009, 2012, 2013). Denitrification via organic material plays a minor role at the study site (Houben, 2000).

The results of Houben et al. (2001) form the baseline for the present study. They go back to analyses carried out mostly at the Technical University (RWTH) of Aachen, Germany. The results of the 2017/2018 resampling, as described in detail below, were obtained at the laboratories of the Federal Institute for Geosciences and Natural Resources (BGR) and the State Authority for Mining, Energy and Geology (LBEG), both in Hanover, Germany.

2.2. Core Drilling

Reactive aquifer components were identified and quantified from drill core material (location see Figure 1). At both sites, the new core drillings were located less than 5 m away from the old ones, thus limiting the

Table 1
Methods and Equipment Used for Hydrochemical Analysis

Parameter	1998/1999	2017/2020
	(RWTH Aachen)	(BGR + LBEG)
pH, temperature, redox, electrical conductivity, dissolved oxygen	WTW MultiLine P4: WTW SenTix 41 Ingold Pt 4805-S7/120 WTW TetraCon 325 WTW CellOx 325	WTW SensoLyt 700 IQ DWA1 WTW SensoLyt 700 IQ Pt WTW TetraCon 700 IQ WTW FDO 701 IQ
On-site dissolved gases	-	Ansyco ATEX GA2000
carbonate species	automatic titration (field): Metrohm Titrino 716	automatic titration: Schott Titroline alpha plus
anions	ion chromatography: DIONEX DX 100	ion chromatography: DIONEX ICS - 3000
cations	ICP-AES: Perkin Elmer Plasma 400	ICP-OES: Spectro Ciros CCD
Exchangeable cations (CEC)	ICP-AES: Perkin Elmer Plasma 400	ICP-OES: Thermo Scientific ICAP 6300 DUO
Nonpurgeable organic carbon (NPOC)		Elementar HighTOC II
trace elements	AAS: Perkin Elmer Zeeman 3030, graphite tray	ICP-MS: Agilent 7500
arsenic	Hydride AAS: Perkin Elmer FIAS200	

potential influence of lateral heterogeneity. The drilling technique of the 1998 cores (60 m continuous, 1-m length each) is described in Houben et al. (2017). The 2018 drill cores (18 m, continuous) on the agricultural site were obtained using a continuous flight auger drilling rig, type Wellco-Drill WD500, owned by the State Authority for Mining, Energy, and Geology (LBEG), Hannover, Germany. The cores had a length of 1 m and an outer diameter of 80 mm. The 2018 cores from the forest site were obtained using a GTR 790 by Geotool. They had a length of 1 m and an outer diameter of 60 mm. The final drilling depth was 8 m. Before sampling, the outer layer was scraped off and the sample was collected from the undisturbed inner part.

2.3. Geochemical Analyses

The pH of soil material was determined on a suspension of 50 g solid in 100 mL distilled water, that was shaken for 72 h in sealed bottles (e.g., Thomas, 1996), using a WTW Multi 340i and a Sentix 41 pH probe. For all other methods, samples were oven-dried at 65°C for 72 h and then turned to powder using an agate mortar mill.

Sulfur contents in 1998 were obtained using a LECO S-200 elemental analyzer (LECO, St. Joseph, USA). The 2018 analyses for sulfur and carbon were performed using a LECO CS-444. The organic carbon (C_{org}) content was measured after carbonate dissolution by repeated exposure of the samples to 10% hydrochloric acid at 80°C, until no further carbon dioxide release was observed.

In 1998, the cation exchange capacity (CEC) was determined using a modified calcite-saturated silver-thiourea method after Pleyrier and Juo (1980). For the 2018 cores, CEC was obtained using the copper triethylenetetramine method by Meier and Kahr (1999), modified by Dohrmann and Kaufhold (2009). The cations on the exchange sites were quantified using the equipment shown in Table 1.

The heavy mineral fractions (2018 samples only) were obtained from the grain size fraction 63–400 μm through density separation in liquid sodium polytungstate (density of 2.9 g/cm^3 at 20°C) after Callahan (1987). The heavy minerals were fixed in epoxy resin (Araldite® 2020) and cut and polished (details see Houben et al., 2017). Samples were inspected with an Environmental Electron Scanning Microscope (ESEM, type FEI Quanta 600F, Genesis 4000 EDX system by EDAX) and evaluated using the Mineral Liberation Analysis (MLA) software developed by Gu (2003), which combines backscattered electron (BSE) images with EDX spectra.

2.4. Hydrochemical Analysis

The two multilevel wells were sampled by RWTH Aachen in 1998 and 1999. In 2002 and 2004, they were sampled by the water supply company. Resampling by BGR and LBEG took place in 2017 and 2020. Both sites are comprised of individually drilled observation wells with short screens (2 m). The Reinkingsbusch site has 7, the Düne site 9 (1998), and 10 (since 2017) screens, respectively.

In all cases, the multilevel observations wells were sampled using a submersible Grundfos MP1 pump, at pumping rates between 100 and 200 l/h. Samples were taken after extracting at least three borehole volumes and after stable values for the in-situ parameters (e.g., pH) had been reached. Cation samples were filtered through 0.45- μm syringe filters in the field and acidified to $\text{pH} < 2$ using ultrapure nitric acid (Merck). The analysis techniques employed 1998/99 and 2017/20 are listed in Table 1.

The tritium content of the 2017 and 2020 samples was determined from its decay product $^3\text{Helium}$ (^3He) at the Institute of Environmental Physics at the University of Bremen (details see Sültenfuß et al., 2009). Samples were degassed and stored for around 100 days to accumulate ^3He . Precision is better than 3%, the detection limit is 0.02 TU. For all samples, duplicate samples of 40 cm^3 each were taken in copper tubes.

For the analysis of dissolved nitrogen and argon (2017 samples only), bubble-free groundwater samples were collected in crimped 120-ml bottles without headspace. The gas concentrations were measured using a membrane inlet gas chromatography mass spectrometer custom built by S + H Analytik GmbH. The samples were pumped along a gas-permeable membrane, through which the gases migrated into a sample loop with helium as carrier gas. Nitrogen, argon, and oxygen were separated from water vapor and other gases via a PorapakQ column. The gas mixture was then passed through a mol sieve (5 Å) to separate N_2 , Ar, and O_2 . Detection and quantification was performed with a Thermo Scientific ISQ Single quadrupole mass spectrometer. Tap water, equilibrated with ambient air at known temperature and pressure, was used for calibration (more details see Houben et al., 2018).

Dissolved chlorofluorocarbon (CFC) concentrations for age dating were measured in 1998 by Spurenstofflabor Dr. Oster, Wachenheim, Germany (for details see Oster et al., 1996).

Two-dimensional reactive transport modeling was done using the PHT3D code (Prommer & Post, 2010) to assess the velocity of the nitrate reduction front. The model was oriented parallel to the main direction of flow, which was calculated using a calibrated three-dimensional regional groundwater flow model. The details of the flow model are provided in the Supporting Information S1. Flow paths were calculated using backward particle tracking from the locations of the observation well screens. The calculated flow paths were used to orient the cross-sectional 2D model and to determine its required length, which was 1,600 m. The cross-sectional model had 160 columns ($\Delta x = 10$ m) and a thickness of 60 m, subdivided into 60 layers ($\Delta z = 1$ m). The hydraulic properties and recharge rates from the regional flow model were projected onto the nodes of the cross-section model. Specified head boundaries were used at the upstream and downstream boundaries, which were taken from the nearest node in the regional flow model. A comparison between the three-dimensional flow paths from the regional flow model and the flowpaths calculated for the cross-sectional model show a good resemblance and only minor deviations of the three-dimensional flow paths from the x - z plane (see animation and Figure S6). The temporal variation of the nitrate concentration of the recharge water was based on a reconstruction of the nitrate input history, which will be detailed in Section 4.2. For SO_4 , the input concentrations were based on measured concentrations in rainfall at the nearby Niedersächsischer Landesbetrieb für Wasserwirtschaft, Küsten- und Naturschutz (NLWKN) station in Lingen-Baccum (details see Figure 2). The yearly mean concentrations, multiplied by four to account for evapotranspiration prior to recharge, were used as model input. The input concentrations of Ca, Cl, Fe, K, Mg, Na, and O_2 were based on measured values for the shallow groundwater. The initial pyrite concentration was derived from measured total sulfur contents of the sediment samples (Houben et al., 2017). A dispersivity of 0.1 m was assumed. We used the kinetic rate expression by Williamson and Rimstidt (1994) with the same rate parameters used by Zhang et al. (2013) to model pyrite oxidation in comparable sandy sediments in the Netherlands. For reasons of brevity, the kinetic rate expressions are not repeated here, but details can be found in Zhang et al. (2013). The reduction of sulfate was not considered, as it has been shown to be very persistent due to the slow reaction kinetics (Böttcher et al., 1989).

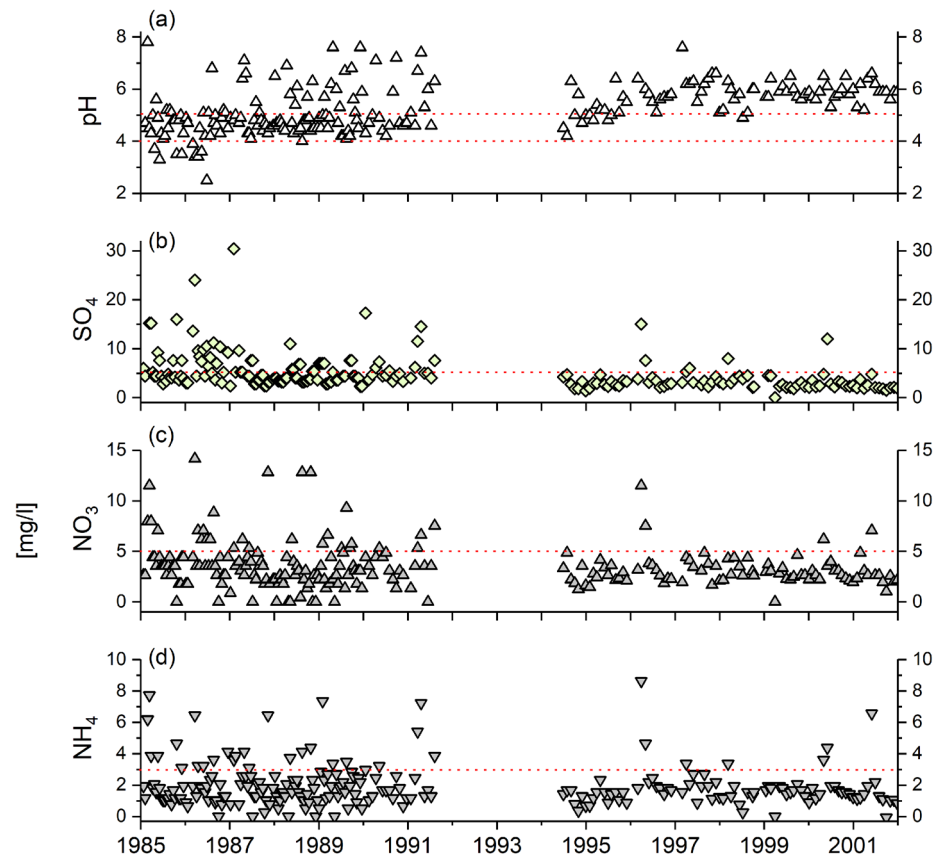


Figure 2. Development of selected rainwater chemistry parameters of biweekly bulk samples 1985–2002 in the Lingen-Baccum weather station (Niedersächsischer Landesbetrieb für Wasserwirtschaft, Küsten- und Naturschutz [NLWKN] station 015, location see Figure 1b): (a) pH, (b) sulfate, (c) nitrate, (d) ammonia. Red dotted lines shown for orientation (data by courtesy of NLWKN). Details on sampling and analysis see NLÖ (1995).

3. Results

3.1. Acidification of Soil and Groundwater in the Reinkingsbusch Forest Site

3.1.1. Development of Rainwater Chemistry

The effects of acidification were already apparent in the forested Reinkingsbusch site with its poorly buffered podzolic soils at the end of the 1990s, as evidenced by elevated dissolved aluminum concentrations and low pH values (Houben et al., 2001). Between 1981 and 1991, sulfur dioxide emissions in Europe decreased by about two thirds, a result of the widespread installation of flue gas desulfurization systems and the relocation of industrial facilities to other continents (Hrkal et al., 2006; Meesenburg et al., 1995). Figure 2 shows that the reduction of atmospheric acid input indeed led to a marked increase of rainwater pH by up to one and a half pH units from around 4.5 in the late 1980s to 6 around the year 2000 (Figure 2a). pH values below 4 did not occur any more after the late 1980s. Sulfate concentrations in rainwater, an indicator of sulfuric acid input, decreased by a factor of two, roughly from averages around 5.0 mg/l in the 1980s to 2.5 mg/l around the year 2000 (Figure 2b). Peak concentrations of above 15 mg/l also disappeared during that period.

Another acid source is ammonia released from agriculture, industry and the combustion of car fuel. In soils and aquifers, it is converted into nitric acid (e.g., Beyn et al., 2014). In central Europe the anthropogenic nitrogen input into the atmosphere decreased by 50% for NO_x and <20% for NH₄ over the past 30 years (e.g., Beyn et al., 2014). In rainwater of the Lingen-Baccum station (Figure 1b), both nitrate (Figure 2c), and ammonia (Figure 2d) do not display a clear trend. While peak concentrations have become less frequent, the bulk concentrations have remained in the same range over the period of observation.

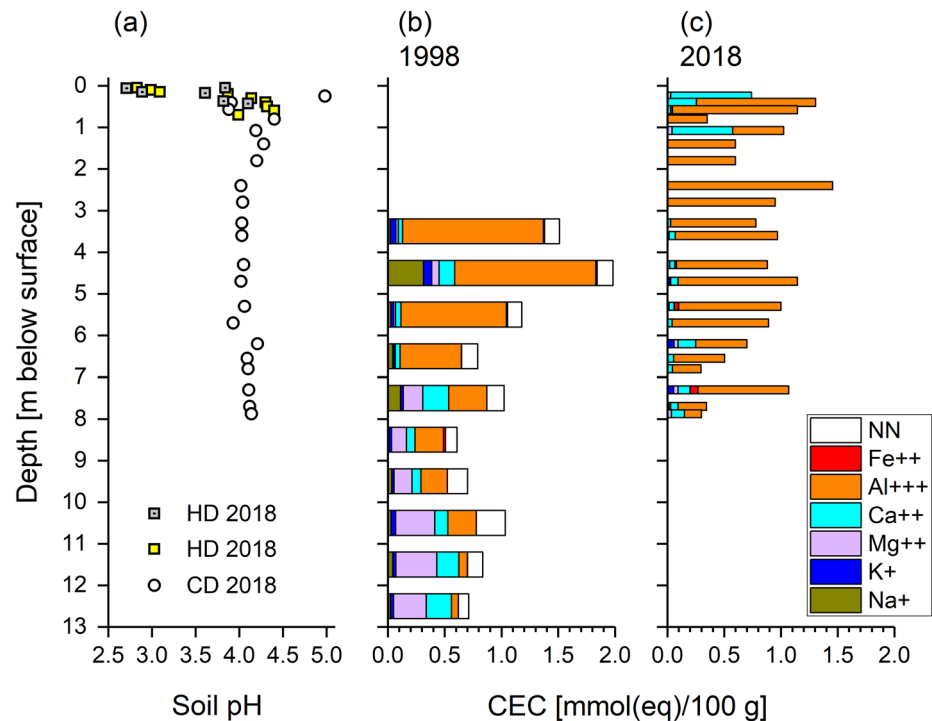


Figure 3. (a) Soil pH as a function of depth at the Reinkingsbusch forest site, hand drilling (HD), core drilling (CD), (b) composition of the cation exchange sites at the Reinkingsbusch forest site for core material 1998 and (c) 2018. NN = unknown if sum of cations < cation exchange capacity (CEC).

3.1.2. Acidification of Soil and Aquifer Material Under the Forest Site

Despite the marked reduction of atmospheric acid deposition, pH values of the top soil of the forest site Reinkingsbusch are still below pH 3 (Figure 3a). The cation exchange capacity of both the 1998 and the 2018 samples is around 1 mmol (eq)/100 g (Figures 3b and 3c), a value typical for sandy sediments. Assuming a porosity of 0.30 and a mineral density of 2.65 g/cm³ (quartz), this value corresponds to 60 mmol (eq) of exchange sites per liter of groundwater. The composition of the exchange sites changed little in the last 20 years: Aluminum is still by far the dominant cation in the upper parts of the soil and groundwater column (Figures 3b and 3c). The aluminum front, however, progressed to some degree. In 1998, the exchange sites were almost exclusively charged with aluminum down to a depth of 6.5 m, in 2018 this is visible down to 8 m, where calcium is still present. The three higher calcium values close to the surface in Figure 3c are attributed to lime application that was conducted during the past years to counteract soil acidification.

3.1.3. Acidification of Groundwater Under the Forest Site

Acidification of groundwater in the forest site has not abated in the uppermost screens, as evidenced by the consistently low pH (Figure 4a). As a result, dissolved aluminum in the top screen have even increased (Figure 4b). Both chloride and sulfate concentrations have decreased somewhat in the two upper screens, which reflects the decrease of atmospheric input (Figures 4c and 4d). Nitrate on the other hand, increased remarkably in the upper 15 m during the last 20 years, with some samples doubling or tripling in concentration compared to 1998 (Figure 4e). Since the nitrogen input from rain has remained stable in the last decades (Figure 2), stable concentrations in groundwater would be expected. The vegetation could play a role here, as pine forests are known for their effective interception of atmospheric pollutants (e.g., Gundersen et al., 2006). The increase is, however, most likely explained by a change of land use. Parts of the forest were cleared at the end of the 1990s to make room for a golf course (Figure 1c). Such clearings can lead to higher nitrate release (e.g., Vitousek, 1981). The created greens might be a source of additional nitrate, due to the use of fertilizer (e.g., Baris et al., 2010; Filipović et al., 2015; Winter & Dillon, 2006). Several of the uppermost samples in Figure 3c have higher calcium concentrations, related to the aforementioned lime

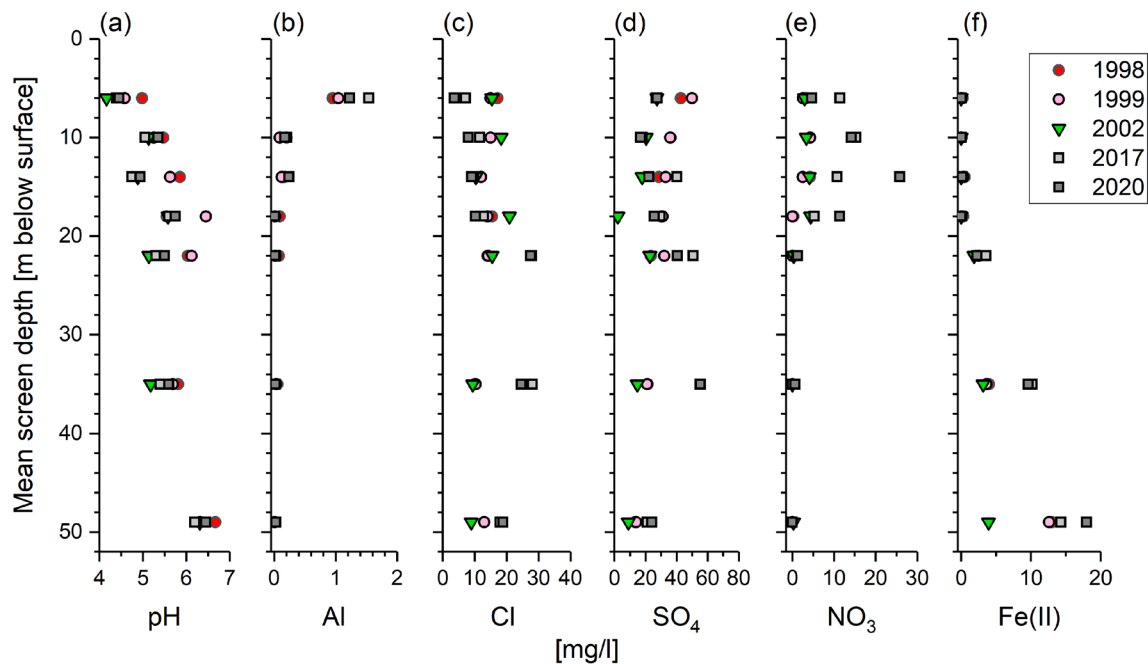


Figure 4. Main hydrochemical parameters of the Reinkingsbusch forest site: (a) pH, (b) aluminum, (c) chloride, (d) sulfate, (e) nitrate, (f) iron.

applications. These could be a cause of nitrate release, since sudden increases of soil pH often induce nitrification and a pulse-like nitrate outwash (e.g., Marschner et al., 1989; Matzner et al., 1983).

3.2. Propagation of the Nitrate Reduction Front in the Agricultural Düne Site

3.2.1. Nitrate Reduction Front Position Based on Analysis of the Aquifer Material

In 1998, the denitrification front was found at a depth of 11.40-m below ground, while in 2018 it was encountered at 11.26 m, indicated by a change from yellow to green colors (Figure 5). Given the disturbance by the core drilling, resulting in differing degrees of compaction of the top soil and core losses, an exact replication of the depth would have been unlikely. The sediments, however, contain a single layer enriched in organic matter, which was used as a marker horizon. The core photographs in Figure 5 were therefore vertically shifted to align the dark-banded horizons of both cores. Taking into account the natural heterogeneity and the associated uncertainty of matching the dark bands, the pictures show no evidence of significant vertical displacement of the redoxline over the 20-year period. Houben et al. (2001, 2017) had predicted a maximum downward propagation of the denitrification front of less than two centimeters over the last 20 years. Such small differences would be difficult to resolve.

The assumption that all sulfur derives from pyrite was deemed valid since oxidized, pyrite-free samples had very low sulfur concentrations and pyrite was found in the heavy mineral fraction only below the redoxline (Figure 6). Interestingly, total sulfur contents seem to have decreased somewhat below the redox front in the last 20 years. Whether this indicates a consumption of pyrite, a natural spatial variation or an analytical uncertainty remains unclear.

3.2.2. Nitrate Reduction Front Position Based on Hydrochemistry

The hydrochemical parameters shown in Figure 7 show generally stable patterns over time. The redoxcline, which is marked by the disappearance of nitrate and oxygen (Figures 7d and 7e) and the increase in sulfate and iron (Figures 7c and 7f) is visible at roughly 12-m depth. Nitrate inputs show a strong temporal fluctuation: the screen at 7 m depth has concentrations varying between almost zero and 125 mg/l. Sulfate concentrations in the upper aquifer were significantly lower in 2017/2020 than in 1998–2004, especially below the redoxline (Figure 7b), but had increased in the deeper aquifer. It should be noted that while the depth

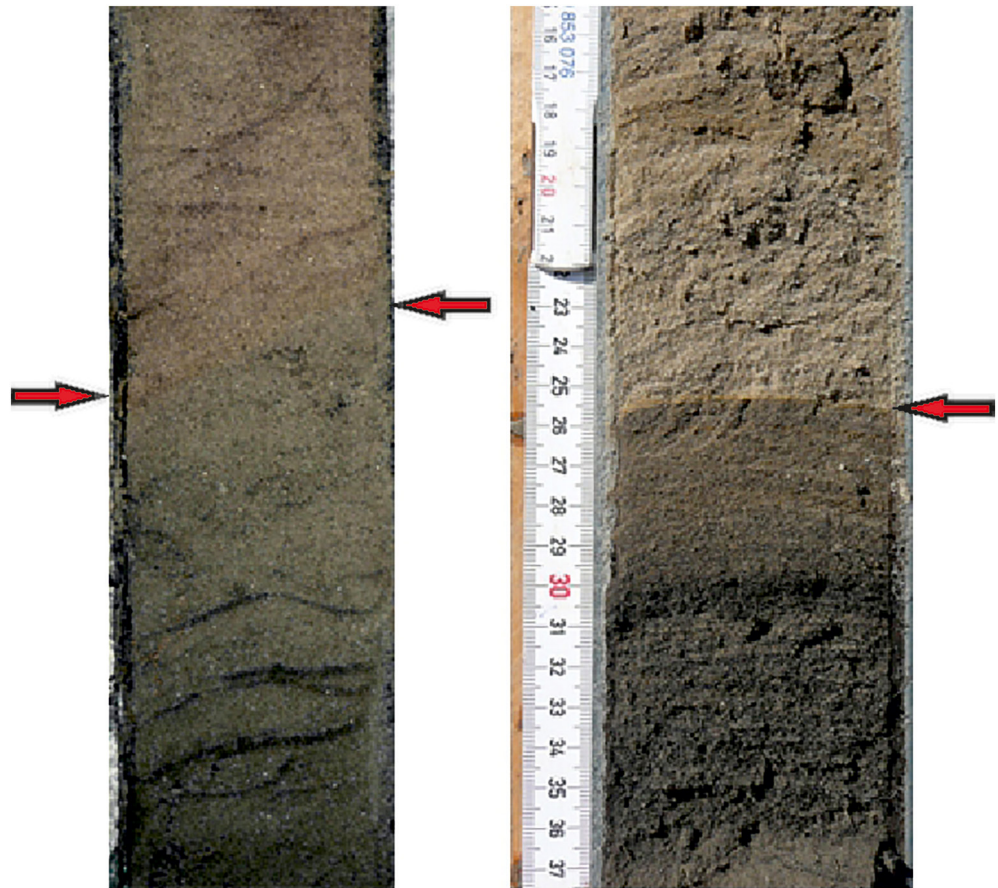


Figure 5. Comparison of drill cores 1998 (left) and 2018 (right) from the agricultural Düne site. The redoxcline (red arrows) is visible as transition from lighter reddish-yellowish to greenish darker colors, with a thin iron oxide band at the top. Please note the dark charcoal bands in the lower half used as marker horizon.

of the redox front can be pinpointed to a few centimeters in the core (Figures 5 and 6), the spatial vertical resolution of the observation wells is much lower due to their screen length (2 m) and gaps in coverage between the screen depths.

The position of the redoxcline is also visible in the dissolved trace element concentrations, especially of the chalcophilic elements related to pyrite (Figures 7g–7m). Concentrations of nickel, cobalt, arsenic, zinc and cadmium above the background occur in a depth interval between 12 and 20–22 m, which is below the zone of lithotrophic denitrification. Lead, which was detected only in a few pyrite crystals by Houben et al. (2017), increased slightly at the redoxcline (Figure 8). Uranium, which occurs in elevated concentrations around lithotrophic denitrification zones in other parts of Germany (van Berk and Fu, 2017), was low (Figure 7m).

Subsurface denitrification will lead to concentrations of dissolved N_2 , normalized for the dissolved concentration of the conservative noble gas argon, exceeding those in pure water in equilibrium with the atmosphere (Fortuin & Willemssen, 2005). Excess nitrogen in the upper aquifer, below the redoxcline, is surprisingly small. In the lower aquifer, however, the N_2/Ar ratios exceed atmospheric equilibrium ratios (Figure 8). The measured dissolved argon concentrations were slightly higher than equilibrium concentrations, indicating the uptake of excess air during groundwater recharge (Figures 8c and 8g).

3.2.3. Development of the Hydrochemistry of the Production Wells

Hydrochemical time series of several production wells, which are located in the immediate vicinity of the Düne and Reinkingsbusch sites (Figure 1c), show an almost continuous increase of ferrous iron and sulfate,

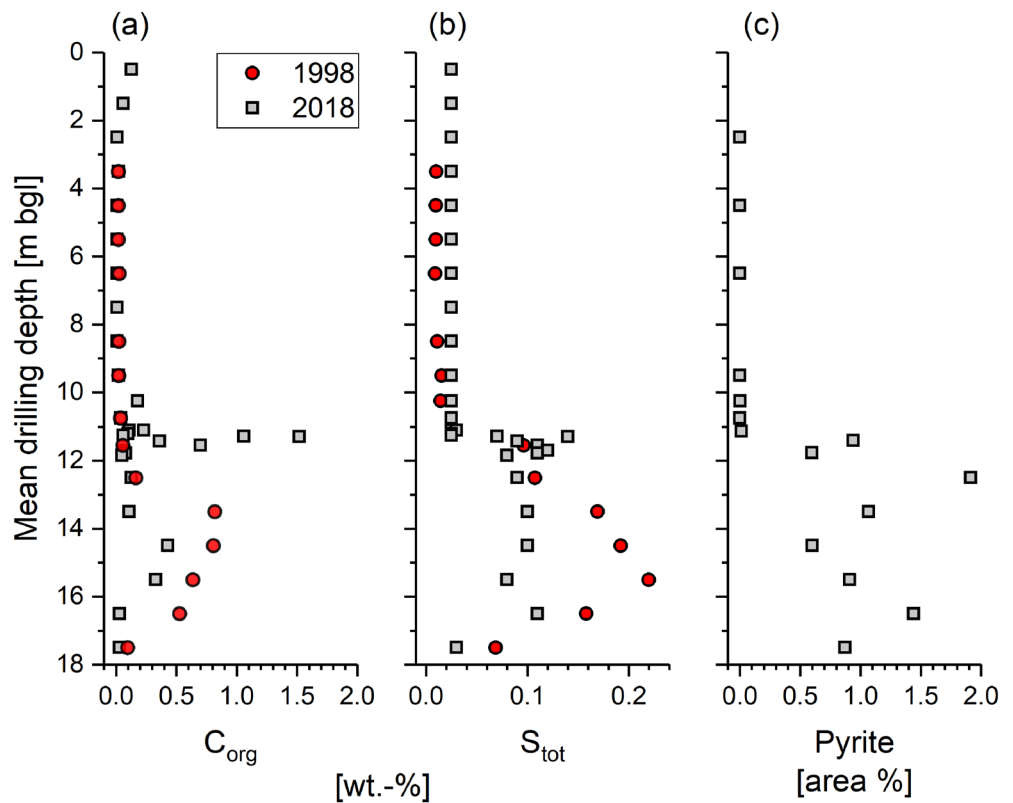


Figure 6. Analysis of core material from the agricultural Düne site: (a) organic carbon, (b) total sulfur, (c) pyrite (obtained from separated heavy mineral fraction, 2018 data only).

the reaction products of pyrite oxidation. Figure 9a shows the example of Well VB3 (built in 1971, screened at 49–58 m depth in the lower aquifer). Chloride, a conservative ion, not controlled by lithotrophic denitrification, also increased slightly (Figure 9a). It may stem from agricultural fertilizers (e.g., potassium chloride) and road salt. The molar ratio of sulfate over chloride increased almost linearly (Figure 9b), indicating that sulfate is indeed being produced in the aquifers.

3.3. Comparison of Groundwater Age Data

Both the chlorofluorocarbon and the tritium-helium groundwater ages show a general and more or less linear increase with depth (Figure 10). The aquitard does not cause a significant modification of this pattern. Chlorinated fluorocarbons can be affected by reductive decomposition, especially in the (lithotrophic) denitrification zone (Hinsby et al., 2007; Oster et al., 1996; Sebol et al., 2007), and therefore lead to erroneous apparent groundwater ages. Indeed, the CFC and T-He ages shown in Figure 10 show a good agreement in the oxic zone and some unsystematic deviations in the reducing zone.

Nevertheless, the 1999 CFC-based age profile for the agricultural site shows a plausible age distribution with depth (Figure 10a), yielding a vertical flow velocity of 0.95 m/a and a reasonable recharge rate of 290 mm/a, the latter calculated after Vogel (1967, 1970). The general trend of the 2017 and 2020 tritium-helium ages support this. However, the ages at 17- and 22-m depth indicate the presence of unusually young water at this depth. A possible explanation could be the lateral inflow of young groundwater from sites with different land uses and higher recharge, the latter possibly augmented by increased irrigation in the last years, in response to dry summers.

At the forest site, the correspondence of the ages according to both methods in the upper aquifer is good, and indicates a vertical flow velocity in the upper aquifer of 0.7 m/a (Figure 10b), which corresponds to a recharge rate of 210 mm/a, which is within the range expected for such sites.

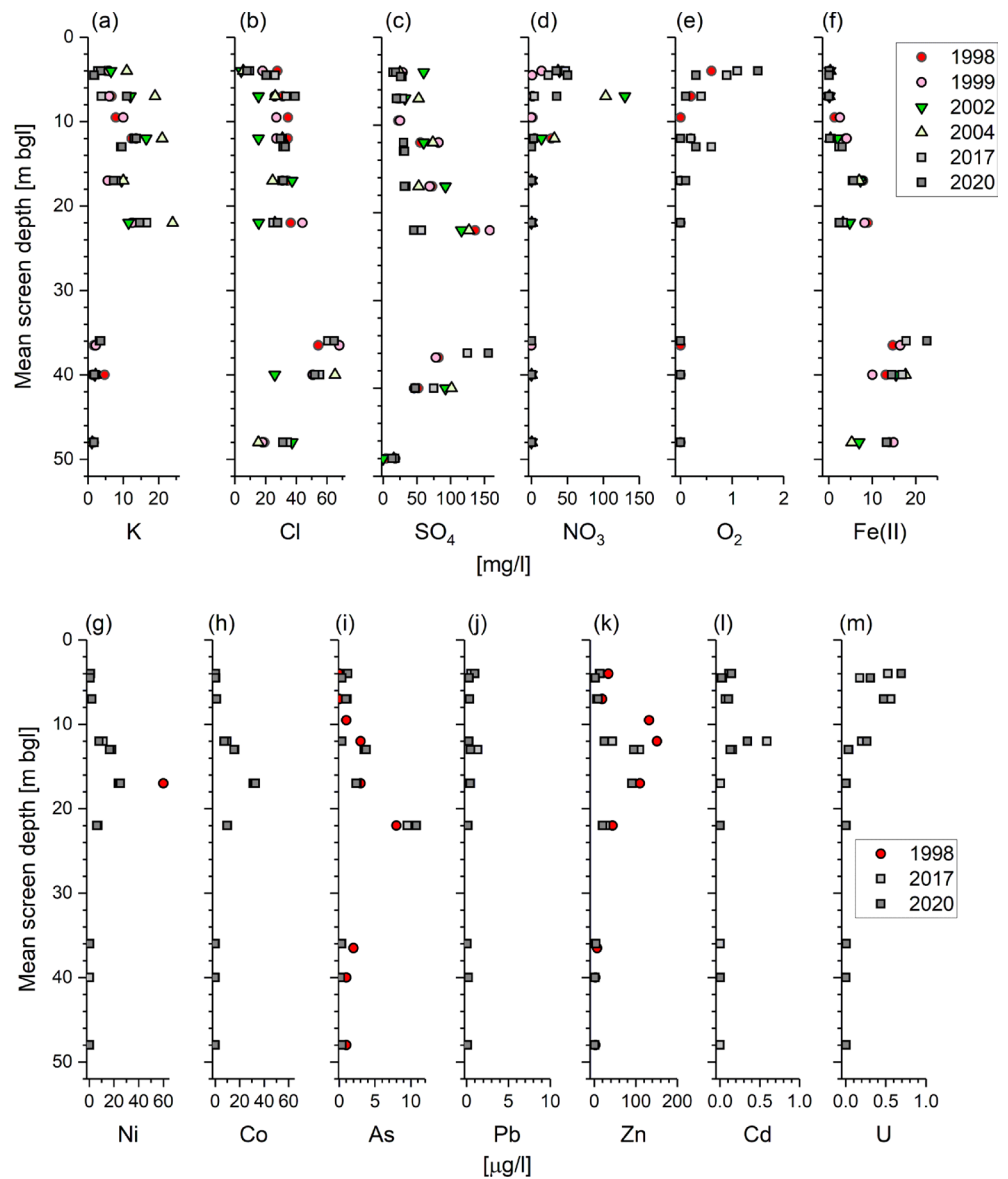


Figure 7. Hydrochemical parameters as a function of depth of the Düne multilevel well (agricultural site): (a) potassium, (b) chloride, (c) sulfate, (d) nitrate, (e) dissolved oxygen, (f) ferrous iron, (g) nickel, (h) cobalt, (i) arsenic, (j) lead, (k) zinc, (l) cadmium, (m) uranium. The detection limit for nickel in 1998 was 20 µg/l (values below not shown). No trace element data for 1999, 2002 and 2004 available.

4. Discussion

4.1. Persistence of Soil and Groundwater Acidification at the Forest Site

The observed persistence of acidification in both soil and groundwater is a legacy of the massive acid inputs of the 1980s, which have exhausted the carbonate buffer capacity of both soil and aquifer material (Figures 3 and 4). The remaining buffers, such as the silicates, are not reactive enough in the present pH range to provide a recovery. Despite the impressive improvement of air quality, rainwater is still slightly acidic, in parts due to the ongoing atmospheric deposition of nitric acid, which has not decreased as much as sulfur deposition (Figure 2). The input of buffering substances through rainwater is therefore far too low to have made an impact in the last 20 years. The single lime application at the Reinkingsbusch site has only marginally improved the situation in the uppermost meters (Figure 3c).

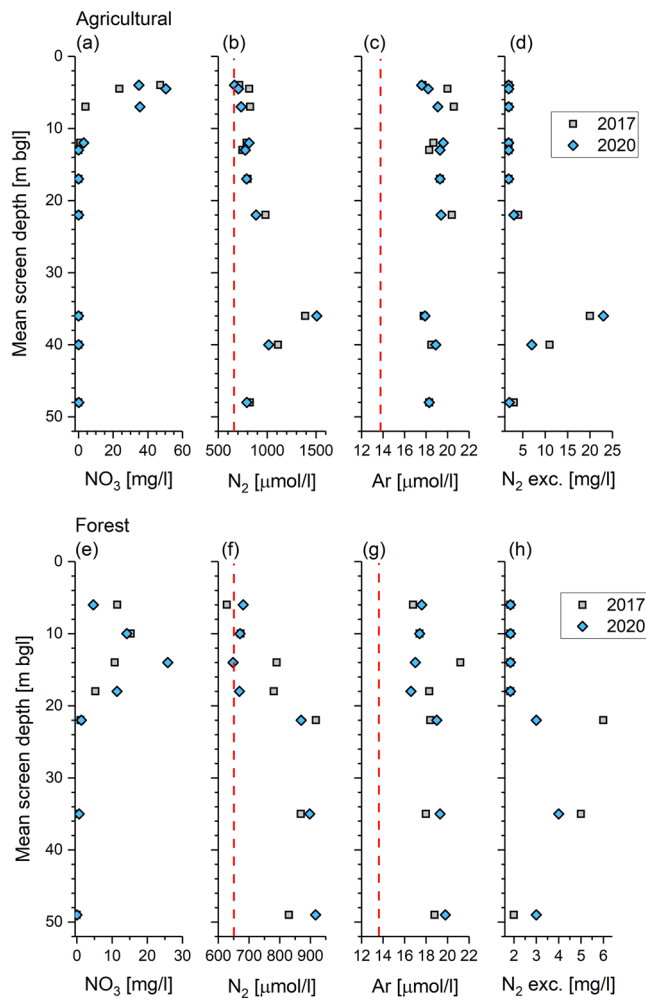


Figure 8. Indicators of denitrification in groundwater (2017 and 2020) as a function of depth: (a, e) nitrate, (b, f) dissolved nitrogen, (c, g) dissolved argon, (d, h) excess nitrogen. The red dashed lines indicate the dissolved gas concentrations at equilibrium (temperature: 10°C, pressure: 1 atmosphere, nitrogen: 647.3 $\mu\text{mol/l}$, argon: 17.23 $\mu\text{mol/l}$).

An exchange complex with a CEC of 60 mmol (eq)/l covered entirely by trivalent aluminum corresponds to a reservoir of 20 mmol (540 mg) of aluminum for each liter of shallow groundwater. Measured dissolved concentrations rarely exceed 3 mg/l (Figures 4b, Houben et al., 2001). Even if the aluminum release would completely stop today, it would require at least 180 flushings of the pore volume at this concentration level to expel the sorbed aluminum. Assuming a mean volumetric soil water content in the unsaturated zone of 10% and a recharge rate of 230 mm/a, the upper meter of soil gets flushed 2.3 times per year, hence the aluminum stored on the exchange sites can sustain the current dissolved aluminum concentrations for almost 80 years, provided the recharge contains sufficient desorbing cations. Column experiments, mass balance calculations and reactive transport models by Houben et al. (2001) already suggested that recovery would require an almost complete removal of aluminum from the exchange sites before an improvement would become noticeable. This shows that groundwater systems recover only very slowly, in the range of decades or centuries, from acid inputs, unless active remediation, such as repeated lime applications, is put in place.

4.2. Propagation of Denitrification Products in Groundwater at the Agricultural Site

Based on stoichiometric mass balance calculations, column experiments on aquifer material cores and 1D hydrogeochemical reactive transport models, Houben et al. (2001) had predicted vertical denitrification front velocities of ca. 0.5–2.0 mm/a. Using a 1D reactive transport model, Houben et al. (2017) calculated velocities up to 8.75 mm/a for low pyrite contents and a continuous high nitrate input of 124 mg/l. The large spread of modeled velocities is a result of the combined effects of the heterogeneity in both nitrate input and pyrite content. The very small displacement of the redox front over the last 20 years (Figure 5) suggests an average downward propagation velocity in the range of 1.0 mm/a, which is well in line with previous estimates. The reason for this relatively slow movement is the comparably high pyrite content of around 0.1–0.2 wt. % (80–160 mmol pyrite per liter of groundwater; Figure 6).

Both the sulfate and excess nitrogen concentrations from Figures 4, 7, and 8, respectively, can be used to infer the historical input of nitrate (for the stoichiometry see e.g., Houben et al., 2001). Each milligram of excess N_2 corresponds to 4.4 mg/l initially present nitrate. The excess values of 5–20 mg/l from Figure 8 thus equal 25–100 mg/l of input nitrate. The sulfate concentrations in the multi-level wells presented in Figure 8 (50–150 mg/l) can also be converted into the amount of nitrate that led to its formation via lithotrophic denitrification (1 mg sulfate \approx 0.9 mg/l nitrate). A natural background sulfate concentration for deeper groundwater of 5 mg/l was assumed, based on Figure 9. This corresponds to nitrate concentrations of the original recharge water of 45–135 mg/l. Both nitrate ranges are quite similar and match the observed peak nitrate concentrations in the upper aquifer in the region (up to 125 mg/l, Houben et al., 2001). The sulfate concentrations of the production wells are much lower (20–70 mg/l, e.g., Figure 9a) due to the dilution caused by long well screens, which also draw in older, nitrate and sulfate-free water. There is, however, no doubt that the trends visible in Figure 9 indicate that (denitrified) water from the nitrate-polluted upper aquifer replenishes the lower aquifer and that the concentrations of iron and sulfate are still rising.

Combining both calculated nitrate inputs with the age data from Figure 10 allows a tentative reconstruction of the nitrate input history as shown in Figure 11. Collectively, the data support a conceptual model in which the agricultural nitrate load peaked in the 1970s and 80s and then dropped off again. This is in good accordance with the agricultural history of the region. Nitrate concentrations were high during the

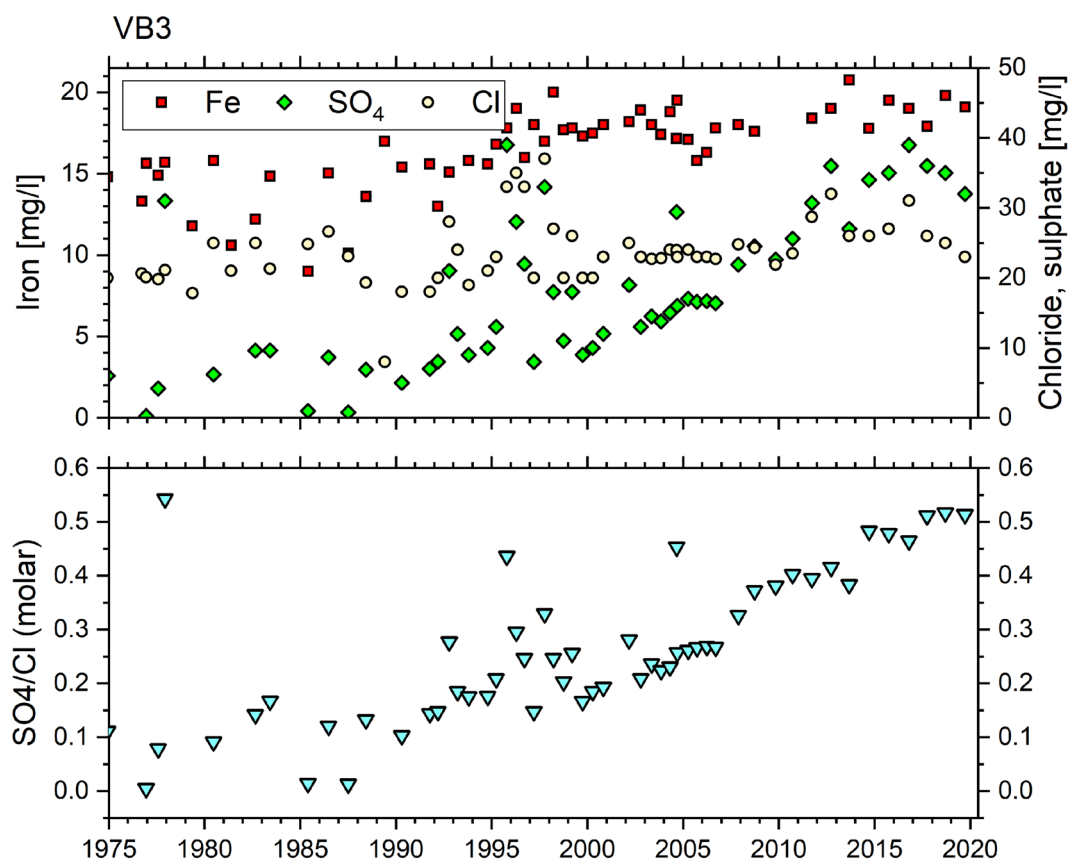


Figure 9. Time series of (a) selected hydrochemical parameters and (b) the molar sulfate to chloride ratio of production well VB3 of the Haren waterworks (location see Figure 1c).

1970/80s, due to the combined effects of deep plowing, dewatering of bog swamps (mineralization of organic material) and a general intensification of agriculture, especially the application of excessive amounts of manure. In the 1980s, the effects of plowing and cultivation had receded and manure and fertilizer application became more strictly regulated (Monteny, 2001; Van Grinsven et al., 2012).

The gap between observation well screens due to the presence of the aquitard precludes constraining a precise input history based on the measured apparent ages. Nevertheless, the increasing sulfate concentration and N₂ excess with depth below the redoxcline, followed by a decrease with depth in the lower aquifer, would be consistent with an increase of nitrate input during, roughly, the 1970s and 1980s, followed by a decrease that would have already started several years before the 1998 data were collected. The high nitrate input would have led to increased pyrite oxidation and thus a pulse of sulfate that has been moving from the redoxcline downward since then. This would also explain the increasing concentrations with depth of Fe, Ni, Co, and As below the redoxcline, albeit that the concentrations of these elements are strongly influenced by other processes, such as sorption (Christensen et al., 1996; Larsen & Postma, 1997). This model would also explain why the N₂/Ar ratio in the deeper aquifer decreases with depth, and is much higher than in the upper aquifer. Finally, the increasing trend of sulfate with time in the production wells is consistent with a sulfate front that has steadily been moving downwards into the upper part of the deep aquifer.

In the reactive transport model, the temporal variation of the nitrate concentration of the recharge water varied according to the red line in Figure 11. It takes into account that (a) nitrate inputs were close to zero before intensive agriculture started in the late 1950s and (b) agricultural practices improved during the 1980s, which led to a reduction in nitrate inputs. A moving average was used to interpolate between the point values, and a constant multiplier of 1.5 was applied to account for the fact that the reconstructed nitrate values are underestimates because of dispersion. While the nitrate input variation is not known with high accuracy, the range employed here is based on time series measurements of shallow groundwater

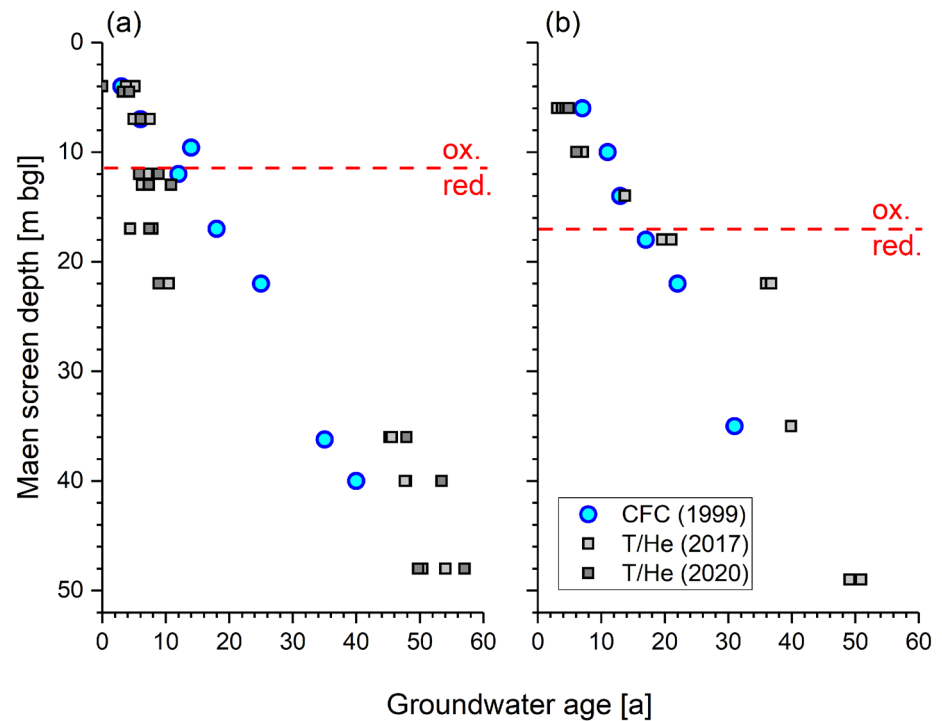


Figure 10. Groundwater ages from chlorofluorocarbon (CFC) (1999) and tritium-helium (2017 and 2020, duplicate samples each) for the (a) agricultural Düne and (b) forest Reinkingsbusch site. The red line indicates the transition from oxic (dissolved oxygen and nitrate present above) to reducing conditions.

concentrations (Figure 7d). The temporal variations are determined by the application regime of manure and fertilizer, crop type, soil turnover rates and weather conditions.

The overall fit of the 2D reactive transport model is good for all six years for which measurements are available (Figure 12). Especially at greater depth, the simulated concentrations of SO_4 and N_2 -excess resemble

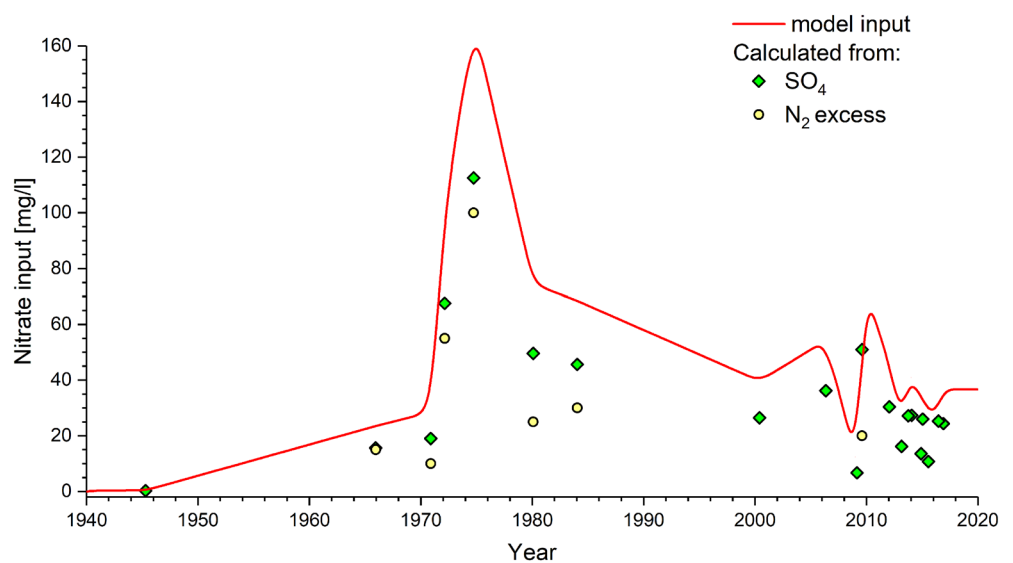


Figure 11. Nitrate input as a function of time, obtained from sulfate and N_2 excess data, using the stoichiometry of lithotrophic denitrification with pyrite, as well as tritium-helium ages (the red curve shows the nitrate input used for the model).

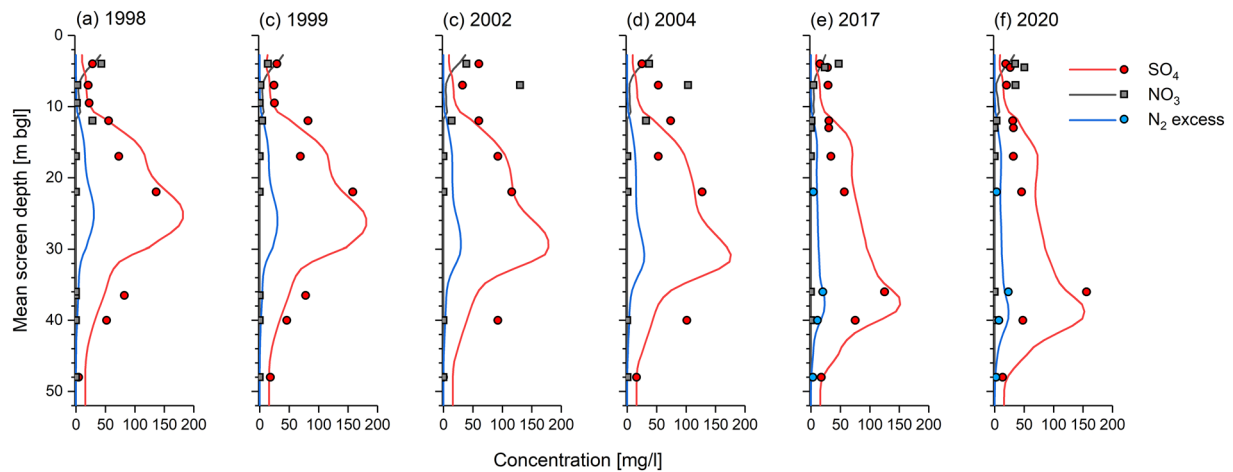


Figure 12. Comparison of the results of the two-dimensional reactive transport model and six years of measured data for the agricultural site (dots = measured data, solid lines = model).

the measured concentrations well. It should be noted that for nitrate, the model is being compared to the data that were used to reconstruct the NO_3 input signal. Nonetheless, the fact that the combination of the pyrite oxidation reaction with the flow regime from the regional flow model produces a compatible pattern, lends credibility to the conceptual model: the currently high SO_4 concentrations and N_2 -excess in the lower aquifer are thus a legacy of the high nitrate load during the 1970s and 1980s. These high loads, as exemplified by the concentrations 2002 and 2004, resulted in a large sulfate bulge between 12 and 30 m depth (Figures 12a–12d). With decreasing nitrate input, sulfate production around the redoxcline declined (Figures 12e and 12f) and the sulfate bulge began moving downwards, toward the pumping wells. Consistent results were obtained by Jessen et al. (2017), who monitored nitrate and sulfate concentrations over a similar timeframe for their test site in Denmark.

In the shallow part of the profile, nitrate concentrations can be seen to increase with depth. In the 1998 data, an increase of nitrate was apparent from the high concentration of the sample at 12 m depth. This pattern is only explainable when it is assumed that the input of nitrate upstream from the multilevel observation well is not uniform in space. Indeed, the road, a strip of trees and a narrow pasture under the management of the drinking water company form a zone with an approximate width of 30 m, with reduced nitrate inputs compared to the arable fields that surround the site. Reducing the nitrate concentration of the recharge water up to 30 m directly upstream from the observation wells in the model led to a marked improvement of the fit between measured and modeled nitrate concentrations. The remaining discrepancies are attributed to the unknown temporal variability of the input signal and local-scale heterogeneities.

5. Conclusions

This study shows the need for long-term monitoring of reaction fronts in groundwater and demonstrates how models can be used to support the data interpretation. The 2017/2020 samplings showed that the general hydrochemical patterns measured in the late 1990s have persisted over nearly 20 years, both for most major ions but also for the trace elements.

Despite the significant decrease of acid and sulfur input from the atmosphere in the last decades, both soil and shallow groundwater at the forest site failed to show improvement with regards to acidification. The main problem lies in the high amount of aluminum sorbed onto the ion exchangers and the exhaustion of the carbonate buffer. A thorough recovery will only occur after the aluminum store has been desorbed and neutralized, as column experiments and reactive transport models by Houben et al. (2001) predicted. The neutralization alone would require a buffering capacity well beyond that of the aquifer material and the rainwater input.

The nitrate reduction front in the upper aquifer has moved very little over the last 20 years. This is due to the relatively high pyrite contents and the markedly decreased nitrate concentrations. Again, this was correctly predicted by previously published one-dimensional reactive transport models (Houben et al., 2001). Groundwater affected by denitrification has already found its way into the lower aquifer, as indicated by steadily increasing sulfate and iron concentrations and N₂ excess values. This was not yet visible in the time series of the late 1990s, which underlines the importance of long-time monitoring. Combining the hydrochemical trends with groundwater ages allows reconstructing the nitrate input history, which increases the predictive capacity of reactive transport models.

Both for the acidification and the nitrate reduction fronts, the hydrochemical and geochemical analyses performed 20 years later show that the predictions of the front velocities based on reactive transport models were accurate. Such models are therefore a useful water resources management tool. Long-term monitoring remains essential though, as unforeseen future events can render model forecasts invalid, for example, the case of the elevated nitrate concentrations at the forest site.

Data Availability Statement

The data used in this study are available in spreadsheet format in the Harvard Dataverse (<https://dataverse.harvard.edu/dataset.xhtml?persistentId=doi:10.7910/DVN/BCG2H5>).

Acknowledgments

The authors would like to thank the Trink- und Abwasserverband Bourtanger Moor, Geeste, Germany, for their technical support. The provision of rainwater chemistry data by NLWKN is gratefully acknowledged. They thank Franziska Holst for the preparation of Figure 1.

References

- Appelo, C. A. J. (1985). CAC. Computer aided chemistry, or simulation of groundwater composition with a geochemical model. *H2O*, 18, 557–562.
- Baris, R. D., Cohen, S. Z., Barnes, N. L., Lam, J., & Ma, Q. (2010). Quantitative analysis of over 20 years of golf course monitoring studies. *Environmental Toxicology & Chemistry*, 29, 1224–1236.
- Beyn, F., Matthias, V., & Dähnke, K. (2014). Changes in atmospheric nitrate deposition in Germany: An isotopic perspective. *Environmental Pollution*, 194, 1–10. <https://doi.org/10.1016/j.envpol.2014.06.043>
- Böhlke, J. K., Wanty, R., Tuttle, M., Delin, G., & Landon, M. (2002). Denitrification in the recharge area of a transient agri-cultural nitrate plume in a glacial outwash sand aquifer, Minnesota. *Water Resources Research*, 38, 1–23. <https://doi.org/10.1029/2001wr000663>
- Böttcher, J., Strebel, O., & Duynisveld, W. H. M. (1989). Kinetik und Modellierung gekoppelter Stoffumsetzungen im Grundwasser eines Lockergesteins-Aquifers. *Geologisches Jahrbuch C*, 51, 23–40.
- Böttcher, J., Strebel, O., Voerkelius, S., & Schmidt, H.-L. (1990). Using isotope fractionation of nitrate-nitrogen and nitrate-oxygen for evaluation of microbial denitrification in a sandy aquifer. *Journal of Hydrology*, 114, 413–424. [https://doi.org/10.1016/0022-1694\(90\)90068-9](https://doi.org/10.1016/0022-1694(90)90068-9)
- Bouwman, A. F., van Vuuren, D. P., Derwent, R. G., & Posch, M. (2002). A global analysis of acidification and eutrophication of terrestrial ecosystems. *Water Air and Soil Pollution*, 141, 349–382. <https://doi.org/10.1023/a:1021398008726>
- Callahan, J. (1987). A nontoxic heavy liquid and inexpensive filters for separation of minerals grains. *Journal of Sedimentary Petrology*, 57, 765–766. <https://doi.org/10.1306/212f8c1a-2b24-11d7-8648000102c1865d>
- Casparie, W. A. (1993). The Bourtanger Moor: Endurance and vulnerability of a raised bog system. *Hydrobiologia*, 265, 203–215. <https://doi.org/10.1007/bf00007269>
- Christensen, T. H., Lehmann, N., Jackson, T., & Holm, P. E. (1996). Cadmium and nickel distribution coefficients for sandy aquifer material. *Journal of Contaminant Hydrology*, 24, 75–84. [https://doi.org/10.1016/0169-7722\(96\)00012-5](https://doi.org/10.1016/0169-7722(96)00012-5)
- Dohrmann, R., & Kaufhold, S. (2009). Three new, quick CEC methods for determining the amounts of exchangeable calcium cations in calcareous clays. *Clays and Clay Minerals*, 57, 338–352. <https://doi.org/10.1346/ccmn.2009.0570306>
- Engesgaard, P., & Kipp, K. L. (1992). A geochemical transport model for redox-controlled movement of mineral fronts in ground water flow systems: A case of nitrate removal by oxidation of pyrite. *Water Resources Research*, 28, 2829–2843. <https://doi.org/10.1029/92wr01264>
- Filipović, V., Toor, G. S., Ondrašek, G., & Kodešová, R. (2015). Modeling water flow and nitrate–nitrogen transport on golf course under turfgrass. *Journal of Soils and Sediments*, 15, 1847–1859.
- Fortuin, N. P. M., & Willemsen, A. (2005). Exsolution of nitrogen and argon by methanogenesis in Dutch ground water. *Journal of Hydrology*, 301, 1–13. <https://doi.org/10.1016/j.jhydrol.2004.06.018>
- Franken, G., Postma, D., Duijnsveld, W. H. M., Böttcher, J., & Molson, J. (2009). Acid groundwater in an anoxic aquifer: Reactive transport modelling of buffering processes. *Applied Geochemistry*, 24, 890–899. <https://doi.org/10.1016/j.apgeochem.2009.02.001>
- Frind, E., Duijnsveld, W. H. M., Strebel, O., & Boettcher, J. (1990). Modeling of multicomponent transport with microbial transformation in groundwater: The Fuhrberg case. *Water Resources Research*, 26, 1707–1719. <https://doi.org/10.1029/wr026i008p01707>
- Galloway, J. N., Likens, G. E., & Edgerton, E. S. (1976). Acid precipitation in the Northeastern United States: pH and acidity. *Science*, 194, 722–724. <https://doi.org/10.1126/science.194.4266.722>
- Gu, Y. (2003). Automated scanning electron microscope based mineral liberation analysis. *Journal of Minerals and Materials Characterization and Engineering*, 2, 33–41. <https://doi.org/10.4236/jmmce.2003.21003>
- Gundersen, P., Schmidt, I. K., & Raulund-Rasmussen, K. (2006). Leaching of nitrate from temperate forests: Effects of air pollution and forest management. *Environmental Reviews*, 14, 1–57. <https://doi.org/10.1139/a05-015>
- Haakh, F. (2017). Nitrate pollution in the groundwater resources of the public drinking water supply. *Water Solutions*, 2-2017, 25–35.
- Haverkamp, M. (2011). Binnenkolonisierung, Moorkultivierung und Torfwirtschaft im Emsland unter besonderer Berücksichtigung des südlichen Bourtanger Moores: Entwicklungslinien und Forschungsstand [Internal colonisation, bog cultivation and peat economy in the Emsland district under special consideration of the southern “Bourtanger Moor”: Lines of development and state of research]. *Telma*, 41, 257–282.

- Henriksen, A., & Kirkhusmo, L. A. (1982). Acidification of groundwater in Norway. *Nordic Hydrol*, 13, 183–192. <https://doi.org/10.2166/nh.1982.0015>
- Hinsby, K., Højberg, A. L., Engesgaard, P., Jensen, K. H., Larsen, F., Plummer, L. N., & Busenberg, E. (2007). Transport and degradation of chlorofluorocarbons (CFCs) (2007) Transport and degradation of chlorofluorocarbons (CFCs) in the pyritic Rabis Creek aquifer, Denmark. *Water Resources Research*, 43, W10423. <https://doi.org/10.1029/2006wr005854>
- Houben, G. (2000). Modellansätze zur Prognose der langfristigen Entwicklung der Grundwasserqualität: Fallbeispiel Bourtanger Moor [Model approaches for predicting the long-term development of groundwater quality: The Bourtanger Moor case]. *Aachener Geowissenschaftliche Beiträge*, 36, 1–213.
- Houben, G. J., Kaufhold, S., Dietel, J., Röhm, H., Gröger-Trampe, J., & Sander, J. (2019). Investigation of the source of acidification in an aquifer in Northern Germany. *Environmental Earth Sciences*, 78, 73. <https://doi.org/10.1007/s12665-019-8096-4>
- Houben, G. J., Koeniger, P., Schloemer, S., Gröger-Trampe, J., & Sültenfuß, J. (2018). Comparison of depth-specific groundwater sampling methods and their influence on hydrochemistry, water isotopes and dissolved gases: Experiences from the Fuhrberger Feld, Germany. *Journal of Hydrology*, 557, 182–196. <https://doi.org/10.1016/j.jhydrol.2017.12.008>
- Houben, G. J., Martiny, A., Bäfler, N., Langguth, H.-R., & Plüger, W. L. (2001). Assessing the reactive transport of inorganic pollutants in groundwater of the Bourtanger Moor area (NW Germany). *Environmental Geology*, 41, 480–488.
- Houben, G. J., Sitnikova, M. A., & Post, V. E. A. (2017). Terrestrial sedimentary pyrites as a potential source of trace metal release to groundwater: A case study from the Emsland, Germany. *Applied Geochemistry*, 76, 99–111. <https://doi.org/10.1016/j.apgeochem.2016.11.019>
- Hrkal, Z. (2001). Vulnerability of groundwater to acid deposition, Jizerské Mountains, northern Czech Republic: Construction and reliability of a CIS-based vulnerability map. *Hydrogeology Journal*, 9, 348–357. <https://doi.org/10.1007/s100400100141>
- Hrkal, Z., Prchalová, H., & Fottová, D. (2006). Trends in impact of acidification on groundwater bodies in the Czech Republic; an estimation of atmospheric deposition at the horizon 2015. *Journal of Atmospheric Chemistry*, 53, 1–12. <https://doi.org/10.1007/s10874-006-0911-0>
- Jessen, S., Postma, D., Thorling, L., Müller, S., Leskelä, J., & Engesgaard, P. (2017). Decadal variations in groundwater quality: A legacy from nitrate leaching and denitrification by pyrite in a sandy aquifer. *Water Resources Research*, 53, 184–198. <https://doi.org/10.1002/2016wr018995>
- Jia, X., Hou, D., Wang, L., O'Connor, D., & Luo, J. (2020). The development of groundwater research in the past 40 years: A burgeoning trend in groundwater depletion and sustainable management. *Journal of Hydrology*, 587, 125006. <https://doi.org/10.1016/j.jhydrol.2020.125006>
- Johnson, N. M., Driscoll, C. T., Eaton, J. S., Likens, G. E., & McDowell, W. H. (1981). Acid rain, dissolved aluminum and chemical weathering at the Hubbard Brook Experimental Forest, New Hampshire. *Geochimica et Cosmochimica Acta*, 45, 1421–1437. [https://doi.org/10.1016/0016-7037\(81\)90276-3](https://doi.org/10.1016/0016-7037(81)90276-3)
- Juncher Jorgensen, C., Jacobsen, O., Elberling, B., & Aamand, J. (2009). Microbial oxidation of pyrite coupled to nitrate reduction in anoxic groundwater sediment. *Environmental Science & Technology*, 43, 4851–4857.
- Keller, W. D., & Smith, G. E. (1967). Ground-water contamination by dissolved nitrate. *Special Paper of the Geological Society of America*, 90, 47–60. <https://doi.org/10.1130/spe90-p47>
- Kölle, W., Strebel, O., & Böttcher, J. (1982). Formation of sulfate by microbial denitrification in a reducing aquifer. *Water Supply*, 3, 35–40.
- Korom, S. F. (1992). Natural denitrification in the saturated zone: A review. *Water Resources Research*, 28, 1657–1668. <https://doi.org/10.1029/92wr00252>
- Larsen, F., & Postma, D. (1997). Nickel mobilization in a groundwater well field: Release by pyrite oxidation and desorption from manganese oxides. *Environmental Science & Technology*, 31, 2589–2595. <https://doi.org/10.1021/es9610794>
- Lee, J. J., & Weber, D. E. (1982). Effects of sulfuric acid rain on major cation and sulfate concentrations of water percolating through two model hardwood forests. *Journal of Environmental Quality*, 11, 57–64. <https://doi.org/10.2134/jeq1982.00472425001100010015x>
- Luehr, H.-P., & Muschack, W. (1983). *Pollution of groundwater from diffuse sources* (pp. 1171–1184). IAHS-AISH Publ.
- Lükewille, A., & van Breemen, N. (1992). Aluminium precipitates from groundwater of an aquifer affected by acid atmospheric deposition in the Senne, Northern Germany. *Water Air and Soil Pollution*, 63, 411–416. <https://doi.org/10.1007/bf00475506>
- Marschner, B., Stahr, K., & Renger, M. (1989). Potential hazards of lime application in a damaged pine forest ecosystem in Berlin, Germany. *Water, Air, and Soil Pollution*, 48, 45–57. <https://doi.org/10.1007/bf00282369>
- Matzner, E., Khanna, P. K., Meiwes, K. J., & Ulrich, B. (1983). Effects of fertilization on the fluxes of chemical elements through different forest ecosystems. *Plant and Soil*, 74, 343–358. <https://doi.org/10.1007/bf02181352>
- Meesenburg, H., Meiwes, K. J., & Rademacher, P. (1995). Long term trends in atmospheric deposition and seepage output in northwest German forest ecosystems. *Water Air and Soil Pollution*, 85, 611–616. <https://doi.org/10.1007/bf00476896>
- Meier, L. P., & Kahr, G. (1999). Determination of the cation exchange capacity (CEC) of clay minerals using the complexes of Copper (II) ion with triethylenetetramine and tetraethylenepentamine. *Clays and Clay Minerals*, 47, 386–388. <https://doi.org/10.1346/ccmn.1999.0470315>
- Monteny, G. J. (2001). The EU nitrates directive: A European approach to combat water pollution from agriculture. *Scientific World*, 1(S2), 927–935. <https://doi.org/10.1100/tsw.2001.377>
- NLÖ. (1995). *Belastungen von Wasser und Boden durch Schadstoffe in Luft und Niederschlägen: Bestandsaufnahme und Konzept für ein Untersuchungs- und Forschungsprogramm [Contamination of soil and groundwater by pollutants in air and precipitation: Inventory and concept for an investigation and research program]* (2nd ed., p. 99). Hildesheim.
- Oster, H., Sonntag, C., & Münnich, K. O. (1996). Groundwater age dating with chlorofluorocarbons. *Water Resources Research*, 32, 2989–3001. <https://doi.org/10.1029/96wr01775>
- Overrein, L. N. (1983). Acid precipitation: An international environmental problem. *Water Science & Technology*, 15, 1–7. <https://doi.org/10.2166/wst.1983.0092>
- Padilla, F. M., Gallardo, M., & Manzano-Agugliaro, F. (2018). Global trends in nitrate leaching research in the 1960–2017 period. *The Science of the Total Environment*, 643, 400–413. <https://doi.org/10.1016/j.scitotenv.2018.06.215>
- Pleysier, J. L., & Juo, A. S. R. (1980). Single-extraction method using silver-thiourea for measuring exchangeable cations and effective CEC in soils with variable charges. *Soil Science*, 129, 205–211. <https://doi.org/10.1097/00010694-198004000-00002>
- Postma, D., Boesen, C., Kristiansen, H., & Larsen, F. (1991). Nitrate reduction in an unconfined aquifer: Water chemistry, reduction processes and geochemical modeling. *Water Resources Research*, 27, 2027–2045. <https://doi.org/10.1029/91wr00989>
- Prommer, H., & Post, V. E. A. (2010). *PHT3D - A reactive multicomponent transport model for saturated porous media, user's manual version 2.10*. Retrieved from <http://www.pht3d.org>
- Rivett, M. O., Buss, S. R., Morgan, P., Smith, J. W. N., & Bemment, C. D. (2008). Nitrate attenuation in groundwater: A review of biogeochemical controlling processes. *Water Research*, 42, 4215–4232. <https://doi.org/10.1016/j.watres.2008.07.020>

- Schwan, J. (1987). Sedimentologic characteristics of a fluvial to aeolian succession in Weichselian talsand in the Emsland (F.R.G.). *Sedimentary Geology*, 52, 273–298. [https://doi.org/10.1016/0037-0738\(87\)90065-0](https://doi.org/10.1016/0037-0738(87)90065-0)
- Sebol, L. A., Robertson, W. D., Busenberg, E., Plummer, L. N., Ryan, M. C., & Schiff, S. L. (2007). Evidence of CFC degradation in groundwater under pyrite-oxidizing conditions. *Journal of Hydrology*, 347, 1–12. <https://doi.org/10.1016/j.jhydrol.2007.08.009>
- Singh, B., & Sekhon, G. S. (1979). Nitrate pollution of groundwater from farm use of nitrogen fertilizers: A review. *Agriculture and Environment*, 4, 207–225. [https://doi.org/10.1016/0304-1131\(79\)90022-5](https://doi.org/10.1016/0304-1131(79)90022-5)
- Smith, R. L., Howes, B. L., & Howes, J. H. (1991). Denitrification in nitrate-contaminated groundwater: Occurrence in steep vertical geochemical gradients. *Geochimica et Cosmochimica Acta*, 55, 1815–1825. [https://doi.org/10.1016/0016-7037\(91\)90026-2](https://doi.org/10.1016/0016-7037(91)90026-2)
- Sültenfuß, J., Roether, W., & Rhein, M. (2009). The Bremen mass spectrometric facility for the measurement of helium isotopes, neon, and tritium in water. *Isotopes in Environmental and Health Studies*, 45, 83–95. <https://doi.org/10.1080/10256010902871929>
- Thomas, G. W. (1996). Soil pH and soil acidity. *Methods of soil analysis, Part 3, chemical methods book series, No. 5* (pp. 321–352). Soil Sci. Soc. America.
- Trudell, M. R., Gillham, R. W., & Cherry, J. A. (1986). An in-situ study of the occurrence and rate of denitrification in a shallow unconfined sand aquifer. *Journal of Hydrology*, 83, 251–268. [https://doi.org/10.1016/0022-1694\(86\)90155-1](https://doi.org/10.1016/0022-1694(86)90155-1)
- Vaclavkova, S., Jørgensen, C. J., Jacobsen, O. S., Aamand, J., & Elberling, B. (2014). The importance of microbial iron sulfide oxidation for nitrate depletion in anoxic Danish sediments. *Aquatic Geochemistry*, 20(4), 419–435. <https://doi.org/10.1007/s10498-014-9227-x>
- van Beek, C. G. E. M., Hettinga, F., & Straatman, R. (1989). *The effect of manure spreading and acid deposition upon groundwater quality at Vierlingsbeek, the Netherlands* (pp. 155–162). IAHS Publ.
- van Berk, W., & Fu, Y. (2017). Redox roll-front mobilization of geogenic uranium by nitrate input into aquifers: Risks for groundwater resources. *Environmental Science & Technology*, 51, 337–345. <https://doi.org/10.1021/acs.est.6b01569>
- Van Grinsven, H. J. M., Ten Berge, H. F. M., Dalgaard, T., Fraters, B., Durand, P., Hart, A., et al. (2012). Management, regulation and environmental impacts of nitrogen fertilization in northwestern Europe under the Nitrates Directive: A benchmark study. *Biogeosciences*, 9, 5143–5160. <https://doi.org/10.5194/bg-9-5143-2012>
- Vitousek, P. M. (1981). Clear-cutting and the nitrogen cycle. *Ecological Bulletins*, 33, 631–642.
- Vogel, J. C. (1967). Investigation of groundwater flow with radiocarbon. *International atomic energy agency proceedings series* (pp. 355–368). Vienna.
- Vogel, J. C. (1970). Carbon-14 dating of groundwater. *Proceedings series-international atomic energy agency* (pp. 225–239). Vienna.
- Wilde, S., Hansen, C., & Bergmann, A. (2017). Decreasing denitrification capacity in aquifers: Scaled model-based evaluation. *Grundwasser*, 22, 293–308. <https://doi.org/10.1007/s00767-017-0373-0>
- Williamson, M. A., & Rimstidt, J. D. (1994). The kinetics and electrochemical rate-determining step of aqueous pyrite oxidation. *Geochimica et Cosmochimica Acta*, 58, 5443–5454. [https://doi.org/10.1016/0016-7037\(94\)90241-0](https://doi.org/10.1016/0016-7037(94)90241-0)
- Winter, J. G., & Dillon, P. J. (2006). Export of nutrients from golf courses on the Precambrian Shield. *Environmental Pollution*, 141, 550–554. <https://doi.org/10.1016/j.envpol.2005.08.051>
- Zhang, Y.-C., Prommer, H., Broers, H. P., Slomp, C. P., Greskowiak, J., van der Grift, B., & van Cappellen, P. (2013). Model-based integration and analysis of biogeochemical and isotopic dynamics in a nitrate-polluted pyritic aquifer. *Environmental Science & Technology*, 47, 10415–10422. <https://doi.org/10.1021/es4023909>
- Zhang, Y.-C., Slomp, C., Broers, H. P., Bostick, B., Passier, H. F., Boettcher, M. E., et al. (2012). Isotopic and microbiological signatures of pyrite-driven denitrification in a sandy aquifer. *Chemical Geology*, 300, 123–132. <https://doi.org/10.1016/j.chemgeo.2012.01.024>
- Zhang, Y.-C., Slomp, C. P., Broers, H. P., Passier, H. F., & van Cappellen, P. (2009). Denitrification coupled to pyrite oxidation and changes in groundwater quality in a shallow sandy aquifer. *Geochimica et Cosmochimica Acta*, 73, 6716–6726. <https://doi.org/10.1016/j.gca.2009.08.026>

References From the Supporting Information

- Bakker, M., Post, V., Langevin, C. D., Hughes, J. D., White, J. T., Starn, J. J., & Fienen, M. N. (2016). Scripting MODFLOW Model Development Using Python and FloPy. *Ground Water*, 54(5), 733–739. <https://doi.org/10.1111/gwat.12413>
- Ertl, G., Bug, J., Elbracht, J., Engel, N., & Herrmann, F. (2019). *Grundwasserneubildung von Niedersachsen und Bremen - Berechnungen mit dem Wasserhaushaltsmodell mGROWA18* (p. 54). Hannover: LBEG.
- Langevin, C., Hughes, J., Banta, E. R., Niswonger, R. G., Panday, S., & Provost, A. M. (2017). *Documentation for the MODFLOW 6 groundwater flow model (techniques and methods): U.S. Geological Survey techniques and methods, book 6 chap. A55* (p. 197). <https://doi.org/10.3133/tm6A55>
- LBEG. (2009a). *Hydrogeologische Bohrungen. NIBIS kartenserver*. Retrieved from <https://nibis.lbeg.de/cardomap3/?TH=636>
- LBEG. (2009b). *Höhen und Bathymetrie. NIBIS Kartenserver*. Retrieved from <https://nibis.lbeg.de/cardomap3/#>
- NASA. (2019). *Shuttle radar topography mission*. Retrieved from <https://www2.jpl.nasa.gov/srtm/index.html>
- Pesci, M. (2019). *Numerical modelling of inter-aquifer flow through aquitards – case study of the Bourtangter Moor (Germany)*. Hannover: MSc Thesis, Leibniz University.
- TAV Bourtangter Moor. (2018). *Wasserwerke*. Retrieved from <https://www.tavbm.de/infocenter/wasserversorgung/wasserwerke.html>
- TAV Bourtangter Moor. (2019). *Historie*. Retrieved from <https://www.tavbm.de/infocenter/wirueber-uns/historie.html>
- Todd, D. K., & Mays, L. W. (2005). *Groundwater hydrology* (3rd ed.). New York: Wiley.
- WSV. (2019). *Pegel online*. Retrieved from <http://www.pegelonline.wsv.de/gast/start>